

PROTON ACCELERATION AND HIGH ENERGY DENSITY PHYSICS FROM LASER FOIL INTERACTIONS

P.A. Norreys[#], CCLRC Rutherford Appleton Laboratory, Didcot, Oxfordshire, OX11 0QX, UK.

F.N. Beg, University of California San Diego, 9500 Gilman Dr., La Jolla, CA 92093, USA.

E.L. Clark, Atomic Weapons Establishment, Aldermaston, Reading, Berkshire, RG7 4PR, UK.

M. Tatarakis, Technological Educational Institute of Crete, P.O. Box 1939 IRAKLIO, Crete, Greece.

M. Zepf Queens University Belfast, Belfast BT7 1NN, UK

A.E. Dangor, M. Wei, and K. Krushelnick, Blackett Laboratory, Imperial College London, Prince Consort Road, London SW7 2BZ, UK

Abstract

Our team has provided the first observations of energetic ion beam production from the front and rear surfaces thin foil targets upon irradiation by an intense laser beam in the relativistic regime. We invented a new plasma diagnostic technique in which “layered” track detectors and dosimetry media were used to simultaneously record ion angular emission patterns as well as ion spectral information. These results have led to a large number of further experiments in which similar measurement techniques were used and in which protons have been measured up to 58 MeV. The source and acceleration mechanisms for these proton beams have been extensively investigated. There have also been a number of proposed applications for these ion beams, such as for injectors into subsequent conventional acceleration stages, for probing of dense plasmas and for inertial confinement fusion experiments.

INTRODUCTION

The invention of the technique of chirped pulse amplification has allowed access to the relativistic regime where the oscillatory velocity of an electron in a plane polarised electromagnetic field v_{osc} is close to the speed of light. A large number of applications for the laser pulses have been proposed - most of them rely on accelerating charged particles to high velocities.

When an intense laser beam hits a solid target, fast electrons from the front surface can travel through the target to the rear surface, ionising the hydrogen layer there. Hydrocarbon and water surface contaminants provide the protons for acceleration on both front and rear surfaces of the target. The hot electron cloud there accelerates protons to MeV energies by the formation of an electrostatic sheath [1]. The accelerating electric field is given by

$$E = \frac{T_e}{eC_s t} = \frac{T_e}{eL_n}$$

A similar process occurs on the front surface of the target from returning fast electrons. At the same time,

protons from the front surface of the target are accelerated into the dense plasma by an electrostatic shock associated with hole-boring. The piston velocity v_{piston} is given by

$$v_{piston}/c = [(1+\eta) I / m_i n_i c^3]^{1/2}$$

where I is the intensity on target, η is the fraction of energy absorbed, m_i and n_i are the mass and density of the ions, and c is the speed of light.

Acceleration takes place over 10's of μm with an electric field strength in the order of $E \sim 10^{12}$ V/m. This is to be compared with standard accelerators that have accelerating fields of $E \sim 10^6$ V/m, typical scale 10's of meters.

EXPERIMENTS

We were the first to use a technique of layered radiochromic film and CR-39 plastic nuclear track detectors in our studies [2]. This detector pack gives spatial and spectral information of the emitted protons. Ions deposit energy in the plastic as they pass through and damage the CR39 plastic track detectors. Most energy is deposited just as the proton stops at the Bragg peak. CR39 is “developed” in NaOH solution that etches a pit at the surface of the plastic if a proton was stopped there. Knowledge of the range of protons in CR39 and radiochromic film enables the energy of the etched pits to be determined as the protons pass through one or more layers of CR39 or radiochromic film.

An electrostatic sheath field generated by escaping fast electrons accelerates protons from this surface. Measurements of the proton spectrum show a “thermal” distribution of protons up to maximum energy that is related to the hot electron temperature [3]. Up to 10% of the incident laser energy is deposited in this proton “beam”. The maximum proton energy scaling with irradiance on target (that is related to the fast electron temperature) indicated a transition between classical resonance and ponderomotive absorption for an irradiance $\sim 10^{18}$ $\text{Wcm}^2\mu\text{m}^2$ (see Figure 1) [3][4].

*Work supported by UK Engineering and Physical Sciences Research Council. [#]p.norreys@rl.ac.uk

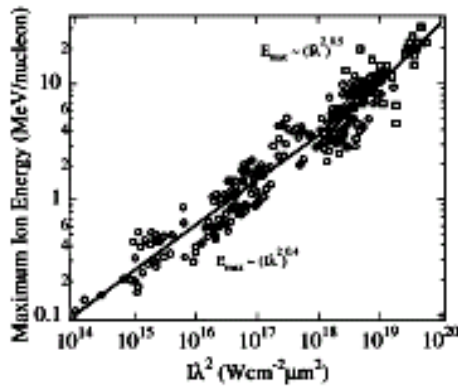


Figure 1: Maximum ion energy against irradiance on target.

In addition, heavy ions were measured using a Thomson parabola and CR-39 detector. Pb^{46+} ion acceleration up to ~ 2 MeV / nucleon has been demonstrated with the Vulcan 100TW facility [4].

It is interesting to note that acceleration in the shock becomes the dominant acceleration mechanism when the protons accelerated there reach the sheath acceleration region at the rear side of the target with a velocity greater than the ions already accelerated in the sheath region. Particle-in-cell modelling by Silva *et al.*, suggests that a signature for this effect is the formation of a plateau region between 15 - 30 MeV. Figure 2 confirms that indeed there is a plateau region up to 15MeV for the higher irradiance on target (110J on target corresponds to an irradiance of $5 \times 10^{19} \text{ Wcm}^{-2} \mu\text{m}^2$ in the focal region).

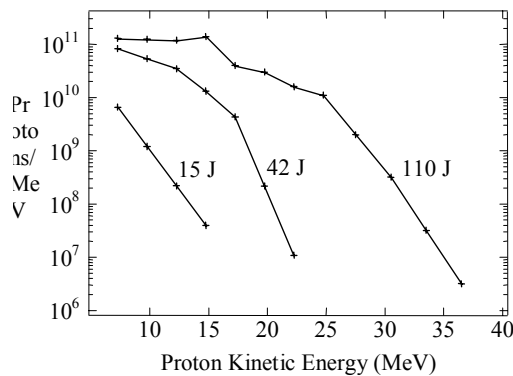


Figure 2: Proton energy spectrum for three shots under identical irradiation conditions, but with increased energy on target.

The initial plasma temperature and target resistivity also plays a significant role in determining which process dominates. Recent 3D tree code simulations of Paul Gibbon show that shock acceleration from the front surface dominates for cold, high resistivity targets [5]. This would correspond to a situation where the fast electron flow is diffusive, rather than free streaming transport behaviour at high intensities, as described by Bell's analytical model [6] and Davies 2D Fokker-Planck simulations [7]. That is to say, when the background resistivity is sufficiently high to prevent the return current compensating the forward fast electron current, the fast electrons cannot propagate freely. Instead, they are trapped 1-2 μm ahead of the ponderomotively driven shock front and act to enhance the electric field there.

Figure 3 shows the proton pattern recorded in CR-39 detectors that show a distinct "ring-like" structure. This was a 100 μm -thick foil irradiated at 10^{19} wcm^{-2} on target. This is confirmation that the ponderomotively driven shock acceleration process dominated for these target and laser conditions [2].

When thin ($< 50 \mu\text{m}$) Al foil targets are irradiated with $5 \times 10^{19} \text{ Wcm}^{-2}$ on target (using the Vulcan 100 TW facility) a uniform poly-energetic proton distribution is observed with no ring structure present. The fact that the ring structure can be reproducibly observed only for "thicker" targets is important evidence that this structure may be due to relatively low fields within the target. This cannot be explained using alternative theories.

It is interesting to note that for shots taken on the Vulcan PW, only those shots with target thickness of 0.5mm showed any clear ring structure in the CR-39 detector. This indicates that sheath acceleration from the rear surface may be dominant for those conditions, in agreement with the observations of Snavely *et al.* [9]. The different pre-pulse duration and intensity conditions between the 100 TW and PW facilities may explain this transition between shock acceleration and rear surface sheath acceleration, as the return current can more easily be supplied by a larger pre-formed plasma. The stretched pulse in the amplifier chain increased from 300 ps to 3 ns between the two laser configurations.

DISCUSSION

Some researchers have suggested that the "ring" structure in the CR-39 is an artefact of overexposure of the track detector. This comment is not relevant to our studies - a simple inspection of the CR-39 confirms that they are not overexposed, except within the ring itself.

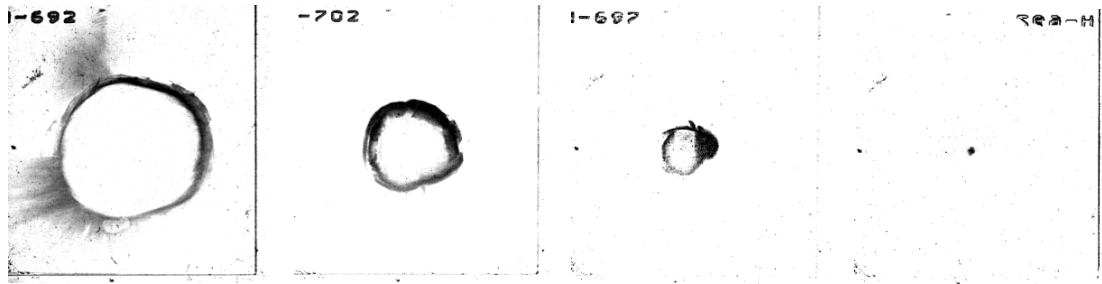


Figure 3: CR-39 track detectors showing a ring-like structure and that the proton beam is emitted in a mono-energetic pattern that is energy dependent.

The observation of energy resolved angular distribution in Figure 3 indicates that it is possible to generate mono-energetic proton beams rather easily with the insertion of a suitably designed spatial filter. These protons could then be used as an injector for subsequent acceleration in a conventional accelerator. Indeed, heavier ions could also be used for this purpose in the future. It is interesting to note that Cowan *et al.* [10] have shown that the emittance of protons from a laser-produced plasma source can have an emittance < 0.004 mm mrad, which is two order of magnitude better than conventional injectors for accelerators.

There are many applications of the proton and ion beams that have been proposed. These include injectors for subsequent conventional accelerators; isotope production for positron emission tomography [11]; fusion evaporation studies [12]; fast neutron radiography of dense materials for inertial confinement fusion studies [13], among others. Clearly, with so many potential applications, it is vital to understand in detail the dependence of the different acceleration mechanisms on the laser and target conditions. We are funded to investigate these effects by the UK research councils and will be undertaking our next experiment in this investigation later this year on the Vulcan PW facility.

The authors thank all the staff at the Central Laser Facility, Rutherford Appleton Laboratory, for their support in the execution of this work.

REFERENCES

- [1] S.C.Wilks *et al.*, Phys. Plasmas **8**, 542 (2001).
- [2] E.L.Clark *et al.*, Phys. Rev. Lett. **84**, 670 (2000).
- [3] A.P.Fews *et al.*, Phys. Rev. Lett. **73**,1801 (1994).
- [4] E.L.Clark *et al.*, Phys. Rev. Lett. **85**, 1654 (2000).
- [5] P.Gibbon (*private communication 2005*).
- [6] A.R.Bell *et al.*, Plasma Phys & Controlled Fusion **39**, 653 (1997).
- [7] J.R.Davies *et al.*, Phys Rev E **56**, 7193 (1997).
- [8] L.O.Silva *et al.* Phys. Rev. Lett. **92**, 015002 (2004).
- [9] R.A.Snavely *et al.*, Phys. Rev. Lett. **85**, 2945 (2000).
- [10] T.Cowan *et al.*, Phys. Rev. Lett., **92**, 204801 (2004).

- [11] P.McKenna *et al.*, Phys. Rev. Lett. **91**, 075006 (2003).

- [12] K.L.Lancaster *et al.*, Phys. Plasmas **11**, 3404 (2004).

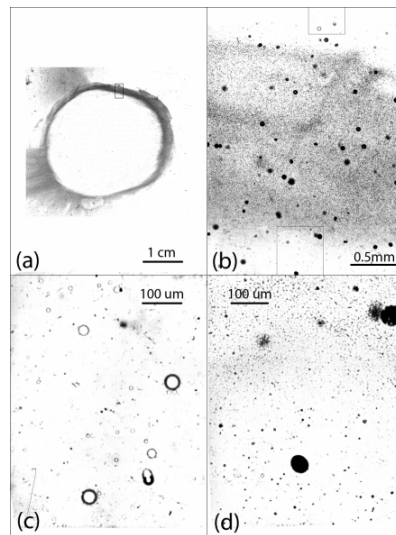


Figure 4: CR-39 detector showing (a) the full pattern (b) a zoomed image of the interior the ring pattern (c) a higher resolution image showing individual $10 \mu\text{m}$ proton pits (d) an image showing heavier ion pits.